Mst1 silencing alleviates hypertensive myocardial injury associated with the augmentation of microvascular endothelial cell autophagy

LING-PENG WANG[1*], RUI-MEI HAN[2*], BIN WU[3*], MENG-YAO LUO[4], YUN-HUI DENG[4], WEI WANG[4], CHAO HUANG[1], XIANG XIE[1] and JIAN LUO[4]

[1]Department of Cardiology, The First Affiliated Hospital, Xinjihypang Medical University, Urumqi, Xinjiang 830000; [2]Department of Cardiology, Shanghai Xuhui Central Hospital, Shanghai 200031; [3]Department of Geriatrics, Xinjiang Military General Hospital; [4]Department of Internal Medicine, The First Affiliated Hospital, Xinjiang Medical University, Urumqi, Xinjiang 830000, P.R. China

Abstract. The activation of mammalian ste20-like kinase1 (Mst1) is a crucial event in cardiac disease development. The inhibition of Mst1 has been recently suggested as a potential therapeutic strategy for the treatment of diabetic cardiomyopathy. However, whether silencing Mst1 also protects against hypertensive (HP) myocardial injury, or the mechanisms through which this protection is conferred are not yet fully understood. The present study aimed to explore the role of Mst1 in HP myocardial injury using *in vivo* and *in vitro* hypertension (HP) models. Angiotensin II (Ang II) was used to establish HP mouse and cardiac microvascular endothelial cell (CMEC) models. CRISPR/adenovirus vector transfection was used to silence Mst1 in these models. Using echocardiography, hematoxylin and eosin staining, Masson's trichrome staining, the enzyme-linked immunosorbent assay detection of inflammatory factors, the enzyme immunoassay detection of oxidative stress markers, terminal deoxynucleotidyl transferase dUTP nick-end labeling staining, scanning electron microscopy, transmission electron microscopy, as well as immunofluorescence and western blot analysis of the autophagy markers, p62, microtubule-associated proteins 1A/1B light chain 3B and Beclin-1, it was found that Ang II induced HP myocardial injury with impaired cardiac function, increased the expression of inflammatory factors, and elevated oxidative stress in mice. In addition, it was found that Ang II reduced autophagy, enhanced apoptosis, and disrupted endothelial integrity and mitochondrial membrane potential in cultured CMECs. The silencing of Mst1 in both *in vivo* and *in vitro* HP models attenuated the HP myocardial injury. On the whole, these findings suggest that Mst1 is a key contributor to HP myocardial injury through the regulation of cardiomyocyte autophagy.

Introduction

Hypertension (HP) is a common condition that accounts for ~12% of primary care consultations globally and is one of the prevailing causes of fatal cardiovascular diseases such as stroke, arrhythmia and ischemic heart disease (1,2). Poor long-term blood pressure management can result in cardiac remodeling, which typically involves cardiomyocyte and endothelial cell apoptosis (3-5). Autophagy has been identified as a pertinent mechanism underlying hypertensive (HP) cardiac diseases (6). Thus, autophagy likely plays a role in cardiac HP, particularly in myocardial microvascular endothelial cells, and may thus be a major contributor to myocardial injury (7-10).

A previous study by the authors demonstrated that the cardiac expression levels of autophagy proteins, including microtubule-associated proteins 1A/1B light chain 3B (LC3), Beclin-1 and autophagy-related 7 (Atg7), were decreased, whereas the expression of p62 was increased in a diabetic mouse model (11). By pharmaceutically restoring the

Correspondence to: Dr Jian Luo, Department of Internal Medicine, The First Affiliated Hospital, Xinjiang Medical University, 137 Liyushan South Road, Urumqi, Xinjiang 830000, P.R. China
E-mail: docsummer@163.com

*Contributed equally

expression of these proteins, cardiac function improved in these mice, further indicating that autophagy is involved in diabetic cardiomyopathy (11). However, the interplay between autophagy and HP myocardial injury, and the underlying mechanisms remain to be fully elucidated.

One candidate protein potentially involved in the interaction between autophagy and HP myocardial injury is mammalian ste20-like kinase1 (Mst1). Mst1 is a protein kinase that can be activated during cardiomyocyte apoptosis (12,13). Exposure to high glucose has been shown to phosphorylate and activate Mst1 in microvascular endothelial cells, leading to apoptosis (12). It has also been shown that decreased autophagy is associated with apoptosis, which is a critical step in the development of diabetic cardiomyopathy (12). The persistent activation of Mst1 has also been observed in dilated cardiomyopathy (DCM) (14). In the present study, it was hypothesized that the inhibition of Mst1 may induce autophagy and confer protective effects against HP-induced myocardial injury. The results obtained using animal and cell HP models suggest that the inhibition of Mst1 can exert protective effects against HP-related cardiomyocyte injuries.

Materials and methods

Mouse model. Mst1 knockout mice (Mst1$^{-/-}$ mice) were purchased from Shanghai Model Organisms. The animals were housed in the SPF animal laboratory of the Animal Experiment Center of Xinjiang Medical University at a constant temperature of 22-24˚C, constant humidity (55±5%), artificial light and dark for 12 h, and free access to water and food. The present study used male Mst1$^{-/-}$ mice and C57BL/6 wild-type (WT) mice (8-10 weeks old, weighing 20-25 g) to establish a mouse model of HP. All experimental mice were randomly allocated into four groups (the control, HP, HP + Ad-KD-Mst1 and HP + Ad-KD-NC groups) with 24 mice in each group. Briefly, Mst1$^{-/-}$ and WT mice in the control groups were subcutaneously infused with 0.9% NaCl using an osmotic bump (ALZET Osmotic Pumps Model 2006, Durect Corp.) for 42 days, and mice in the HP groups were subcutaneously infused with angiotensin II [Ang II; 2,000 ng/kg/min, A604098-0100, Sangon Biotech (Shanghai) Co., Ltd.] for 42 days, as previously described (15,16). In total, 96 mice were used in the experiment. Systolic blood pressure was measured at baseline and during Ang II infusion using a tail-cuff method. A body weight loss >10% was set as the criteria for humane endpoints to remove mice from the experiments. At the end of the experiments, the exsanguination of 100 μl blood from the heart under general anesthesia with 1% pentobarbital sodium (45 mg/kg; P3761, MilliporeSigma) following the collection of the heart was used to euthanize the mice. The body weight of the mice was 30-32 g at the time of sacrifice. The present study was reviewed and approved by Ethics Committee of The First Affiliated Hospital, Xinjiang Medical University (approval no. IACUC20201116-13). All procedures performed in experiments involving animals were in accordance with the ethical standards of the institution or practice at which the studies were conducted.

Cell model. Cardiac microvascular endothelial cells (CMECs; C-12285, PromoCell) were cultured in endothelial cell growth medium MV (C-22020, PromeCell) supplemented with 10% fetal bovine serum (FBS), 100 U/ml penicillin and 100 μg/ml streptomycin at 37˚C in a 5% CO_2 humidified incubator. Ang II (100 μM, 24 h) was used to induce the *in vitro* HP cell model as previously described (17,18). Mst1 silencing was achieved by transfecting Ad-sh-Mst1 [MOI: 200; Hanheng Biotechnology (Shanghai) Co., Ltd.] into the cells. The cultured CMECs were treated with 50 nM bafilomycin A1 (MiilliporeSigma) for 2 h to evaluate the autophagic flux.

Adenovirus construction. The pHBAd-U6-MCS-CMV-GFP-Δloxp was recombined with backbone pBHGlox(delta)E1, 3Cre in bacteria. The adenovirus was packaged using LipofiterTM for 6 h at 37˚C in 293A cells [Hanheng Biotechnology (Shanghai) Co., Ltd.] cultured in Dulbecco's modified Eagle's medium (DMEM) plus 10% FBS, as previously described (19). The nucleotide shRNA of Mst1 was cloned using sequence, 5'-GAAGACTATCGAGGCACAACCAATA-3' and the negative control shRNA sequence was 5'-TTCTCCGAACGTGTC ACGTAA-3'.

Adenovirus transduction. Ad-sh-Mst1 or control Ad-sh-green fluorescent protein (GFP) was designed and provided by Hanheng Biotechnology (Shanghai) Co., Ltd. The titer of the adenoviruses used in the present study was ~1.58x10^{10} PFU/ml. Prior to adenoviral transfection, CMECs (1x10^6 /ml, 3rd generation) were seeded into six-well plates until they reached a confluency of 80%. The cells were then incubated with Ad-sh-Mst1 at an MOI of 200 for 48 h at 37˚C. Fluorescence microscopy was used to observe GFP expression. The mRNA level of Mst1 was further measured to evaluate the effectiveness of adenoviral transfection.

Echocardiography. Transthoracic echocardiography was performed to evaluate mouse cardiac structure and function using a Vevo 2100 ultrasound imaging system (VisualSonics). Briefly, the mice were anesthetized with 1% pentobarbital sodium (45 mg/kg; P3761, MilliporeSigma) and placed on a warmed platform. Ultrasound gel (Ultrasonic coupling agent; TM-100, Tianjin Jinya Electronics Co. Ltd.) was applied to the chest skin after preparation (mice were depilated using the Vetin depilatory cream from the chest to the subxiphoid process up to the left axilla, and the skin was prepared). Subsequently, two-dimensional images and M-mode images of the parasternal short-axis view were recorded using a diagnostic ultrasound machine (Philips HD11 XE). The left ventricular end-diastolic diameter (LVEDD), left ventricular end-systolic diameter (LVESD), left ventricular ejection fraction (LVEF) and left ventricular fractional shortening (LVFS) were then calculated.

Histological analysis. The mouse hearts were harvested and fixed with 10% formalin for 24 h. The hearts were then embedded in paraffin and cut into 5-μm-thick sections. Myocardial morphology and fibrosis were assessed by staining the sections with hematoxylin and eosin (H&E) for 4 min at room temperature, and Masson's trichrome for about 13-15 min at room temperature (D026-1-2; Nanjing Jiancheng Biological Engineering Research Institute Co. Ltd.), respectively, as previously described (20). Images were captured using a light

microscope (E200, Nikon Corporation). The cardiomyocyte size and area of fibrosis were measured using ImageJ software (version 1.50i, National Institutes of Health).

Biochemical assays. Mouse heart samples were homogenized, and supernatants were collected and used for biochemical measurements. The concentrations of interleukin-6 (IL-6; EK206/3-48, Lianke Biotechnology Co., Ltd.), tumor necrosis factor-α (TNF-α; EK282/3-48, EK206/3-48, Lianke Biotechnology), malondialdehyde (MDA; A003-1-1, Nanjing Jiancheng Biological Engineering Research Institute Co. Ltd.), superoxide dismutase (SOD; A001-3-1, Nanjing Jiancheng Biological Engineering Research Institute) and glutathione peroxidase (GSH-PX, A005, Nanjing Jiancheng Biological Engineering Research Institute) were measured using enzyme-linked immunosorbent assays (ELISAs) using commercially available kits (as indicated above) according to the manufacturer's instructions.

Measurement of apoptosis. Apoptotic cells were detected using a terminal deoxynucleotidyl transferase dUTP nick-end labeling (TUNEL) assay kit (MK1015, Boster Biological Technology Co. Ltd.). Briefly, heart paraffin sections were prepared, dewaxed in xylene and hydrated in ethanol. The sections were then incubated for 30 min at 37°C with TUNEL reaction mixture according to the manufacturer's instructions. Images were captured using a fluorescence microscope (E200, Nikon Corporation). TUNEL-positive cells in 10 randomly selected areas were quantified. In total, five visual fields under the microscope were selected randomly to observe the proportion of apoptotic cells in each visual field with the naked eye, and an average apoptotic rate was then calculated using SPSS 19.0 software (IBM Corp. USA).

Microvascular corrosion casting. Microvascular corrosion casting was conducted as previously described (21) using scanning electron microscopy (SEM). Briefly, after being euthanized and perfused, the mice were infused with Mercox CL-2B (Dainippon Ink and Chemicals, Inc.) diluted with monomeric methylmethacrylate (Ladd Research Industries) at a flow rate of 41 ml/h. After the hardening of the injected resin, the heart was washed and submerged in 2% hydrochloric acid. The specimens were then washed, and ice-embedded casts were freeze-dried. The mounted specimens were either evaporated with carbon and gold or sputter-coated with gold and examined using the XL-30 SEM (FEI, Eindhoven) at an accelerating voltage of 10 kV.

Mitochondrial assays. The detection of mitochondrial membrane potential was performed as described previously (22). In brief, the cells were detached using Trypsin (0.25%, #25200-056, Gibco; Thermo Fisher Scientific, Inc.), washed with PBS precooled to 4°C and incubated with JC-1 staining solution for 30 min at 37°C (C2006, Beyotime Institute of Biotechnology). After 30 min, the cells were washed and detected using fluorescence-activated cell sorting (BD LSRFortessa™ System, BD Biosciences). The ratio of red to green fluorescence intensity at an excitation wavelength of 490 nm indicated the mitochondrial membrane potential.

Transmission electron microscopy (TEM) detection of autophagosomes. Autophagosomes were detected using a transmission electron microscope (TEM1230, JEOL, Ltd.) according to a previously published study (23). In brief, cultured CMECs were digested and washed, followed by 2.5% glutaraldehyde fixation at 4°C, and the cells were then examined using an electron microscope. Groups consisting of 10 fields were selected for analysis.

Western blot analyses. The preparation of cell lysates (RIPA buffer, AR0105, Boster Biological Technology) from *in vitro* and *in vivo* samples was performed as previously described (11). Equal amounts (50 μg for tissue lysates or 25 μg for cell lysates) of protein were separated in 10% sodium dodecyl sulfate-polyacrylamide gel electrophoresis and then transferred to polyvinylidene fluoride membranes. The membranes were incubated with antibodies against MST1 (1:1,000, cat. no. 3682S), phosphorylated (p-)Mst1 (1:1,000, cat. no. 49332S), Beclin-1 (1:1,000, cat. no. 3738S), p62 (1:1,000, cat. no. 23214S), LC3B (1:1,000, cat. no. 2775S), cleaved caspase-3 (1:1,000), cleaved caspase-9 (1:1,000), BAX (1:1,000), Bcl-2 (1:1,000), PARP-1 (1:1,000) overnight at 4°C. All primary antibodies were purchased from Cell Signaling Technology, Inc. Following incubation with goat anti-rabbit IgG H&L (conjugated with horseradish peroxidase, 1:5,000, cat. no. ab205718, Abcam) or goat anti-mouse IgG H&L (conjugated with horseradish peroxidase, 1:5,000, cat. no. ab205719, Abcam) for 2 h at room temperature, the bands were detected with enhanced chemiluminescence (SuperSignal West Pico PLUS Chemiluminescent Substrate; cat. no. 34580; Thermo Fisher Scientific, Inc.), and the density and size of the bands were quantified using ImageJ 1.50i software (National Institutes of Health) by normalizing to β-actin [1:1,000, Sangon Biotech (Shanghai) Co., Ltd.] and GAPDH (1:5,000; cat. no. 5174, Cell Signaling Technology, Inc.).

Immunofluorescence. To visualize autophagy markers, the cells were washed with cold phosphate-buffered saline (PBS) and fixed with 4% formaldehyde solution for 20 min. This was followed by permeabilization with 0.5% Triton X-100 for 20 min and incubation with blocking buffer containing 1% bovine serum albumin (BSA) for 30 min at room temperature. Samples were incubated with primary antibodies against LC3B (2 μg/ml, cat. no. 2775S) and p62 (2 μg/ml, cat. no. 23214) (both from Cell Signaling Technology, Inc.) at 37°C for 2 h and secondary antibodies (2 μg/ml, goat anti-rabbit IgG H&L labeled with Alexa Fluor488, cat. no. ab150081, Abcam) at 37°C for 1 h. For myocardial tissue sections, the samples were fixed with acetone at 4°C for 10 min, followed by blocking with 5% BSA for 30 min at room temperature. Incubation with primary antibodies was performed at 4°C overnight and with the secondary antibodies at room temperature for 1 h. Staining without primary antibodies was used as the negative control. Images were obtained using a LSM 700 laser scanning confocal microscope (Carl Zeiss AG).

Statistical analysis. Statistical analyses were conducted using SPSS 19.0 software (IBM Corp.). Data are expressed as the mean ± standard deviation (SD) for the indicated number of experiments or mice. The differences in means between two
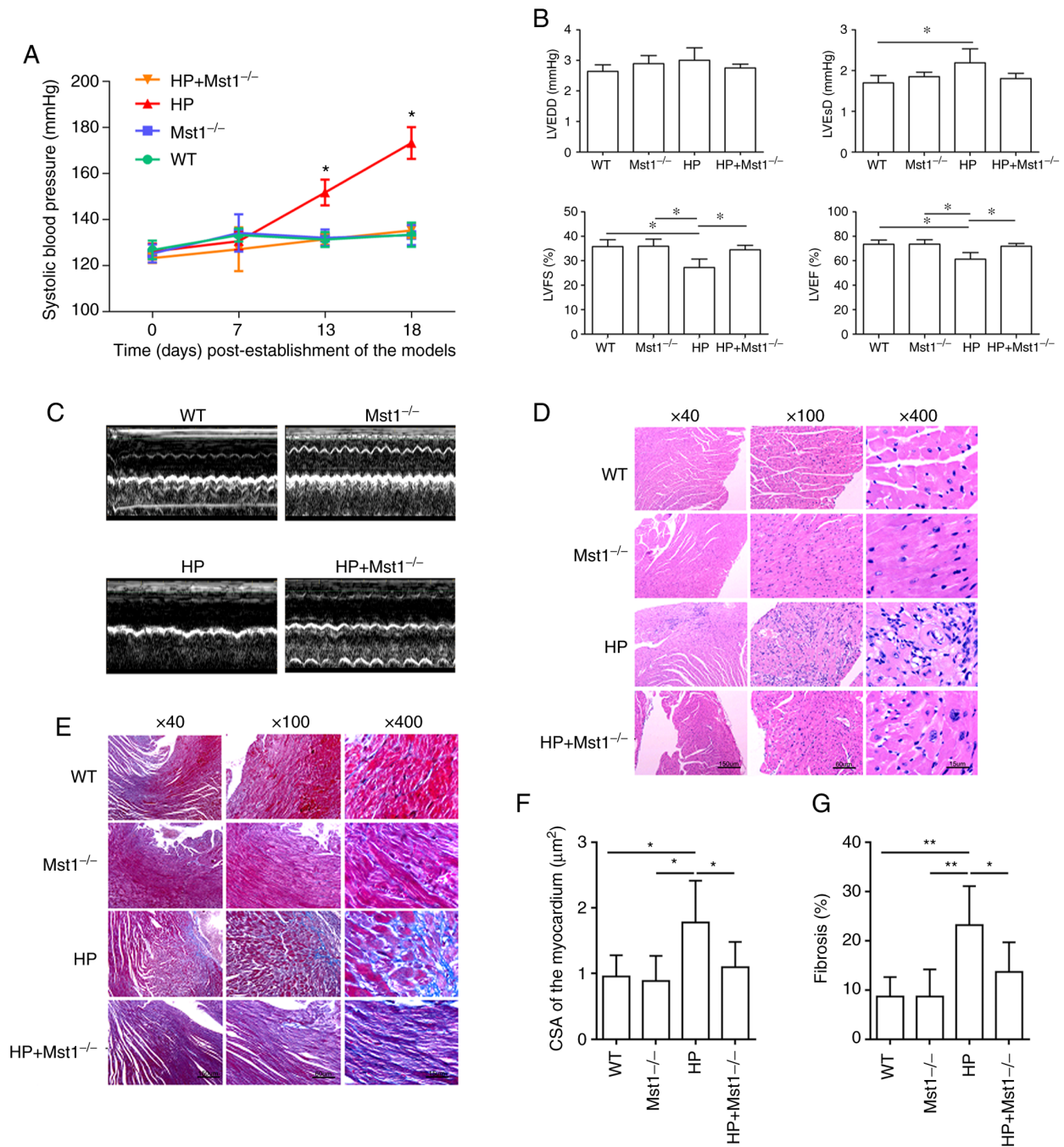
Figure 1. Cardiac morphology and function in mice. (A) Systolic blood pressure of the mice. *P<0.05 vs. WT or Mst1-/-. (B) Representative M-mode echo-cardiography images of WT, Mst1-/-, HP and HP Mst1-/- mice. (C) Quantitative assessment of M-mode images describing left ventricular function; n=6. (D) Representative hematoxylin and eosin staining of mouse cardiac sections. (E) Representative Masson's trichrome staining of mouse cardiac sections. (F) Quantification of cardiomyocyte hypertrophy. (G) Quantification of fibrosis. *P<0.05 and **P<0.01. WT, wild-type; Mst1, mammalian ste20-like kinase 1; HP, hypertensive/hypertension.

groups and multiple groups were evaluated using an unpaired t-test and one-way analysis of variance, respectively. Post-test comparisons for multiple analyses were performed using Tukey's test. P-values were 2-sided and a P-value <0.05 was considered to indicate a statistically significant difference.

Results

Mst1 knockout ameliorates cardiac structure and function in mice with HP. To evaluate the role of Mst1 in the hearts of mice with HP, mouse model of HP was first constructed

as described in the 'Materials and methods'. The knockout of Mst1 significantly attenuated Ang II-induced HP (P<0.05, Fig. 1A). Echocardiography revealed an impaired heart function in the HP group compared to the control group, as indicated by both morphological changes and heart function markers, including LVEDD, LVESD, LVEF and LVFS (all P<0.05, Fig. 1B and C). Mst1 knockout in the HP group resulted in improved cardiac function (all P<0.05, Fig. 1B and C), suggesting a key role of Mst1 in HP. H&E staining (Fig. 1D) and Masson's trichrome staining (Fig. 1E) revealed cardiomyocyte hypertrophy and fibrosis (both P<0.05, Fig. 1F and G) in
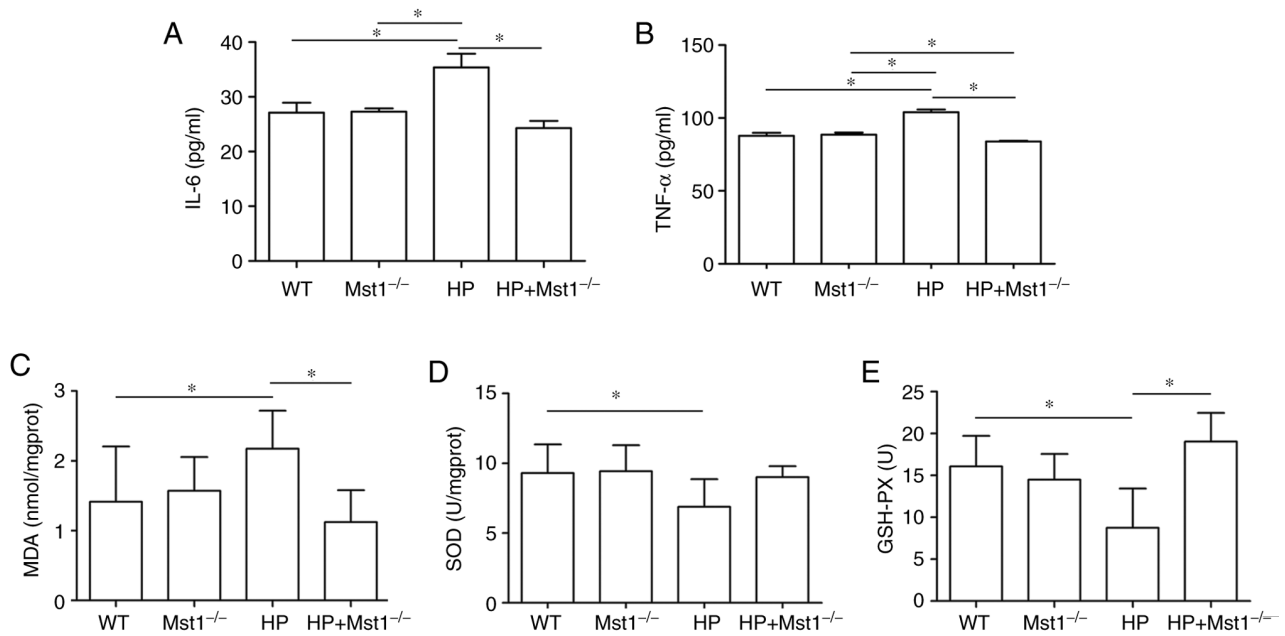
Figure 2. Cardiac levels of inflammatory factors and oxidative stress markers in mice. (A and B) Expression level of IL-6 and TNF-α in mouse myocardium; n=6. (C-E) Protein levels of MDA, SOD and GSH-PX in mouse myocardium; n=6. *P<0.05. IL-6, interleukin-6; TNF-α, tumor necrosis factor-α; MDA, malondialdehyde; SOD, superoxide dismutase; GSH-PX, glutathione peroxidase; WT, wild-type; Mst1, mammalian ste20-like kinase 1; HP, hypertensive/hypertension.
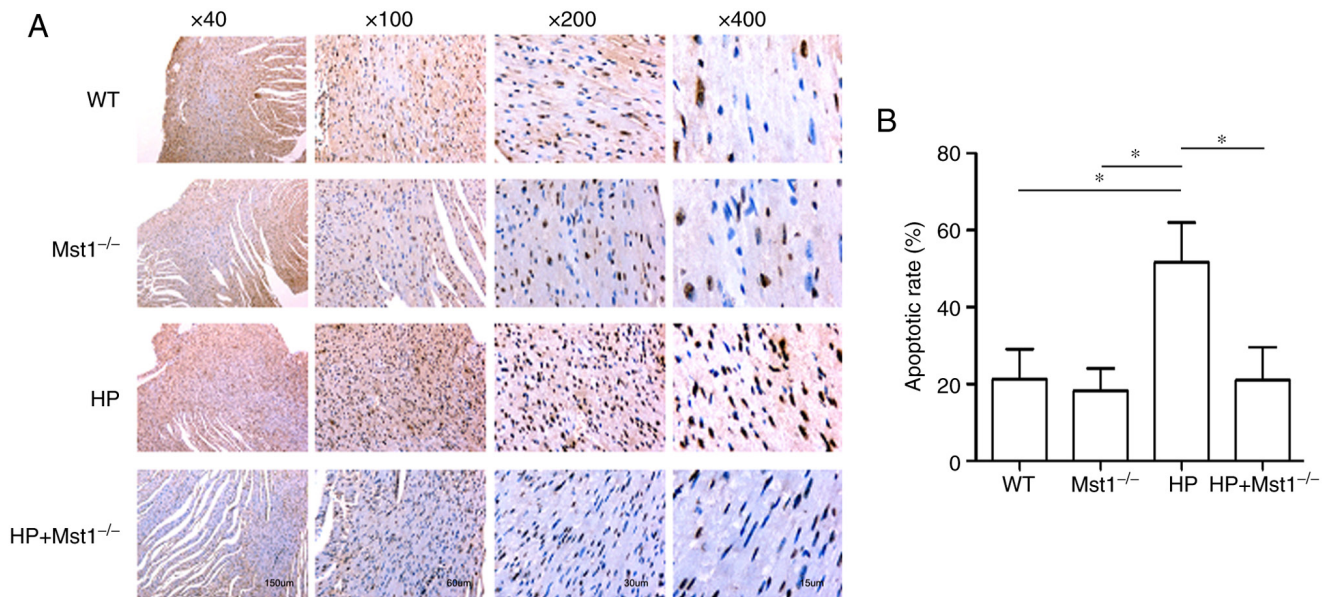

Figure 3. Cardiomyocyte apoptosis in mice. (A) Representative TUNEL staining of mouse cardiac sections. (B) Quantitative assessment of TUNEL staining; n=6. *P<0.05. WT, wild-type; Mst1, mammalian ste20-like kinase 1; HP, hypertensive/hypertension.

the HP group, respectively. Mst1 knockout in the HP group significantly reduced both cardiomyocyte hypertrophy and fibrosis (both P<0.05, Fig. 1D-G), demonstrating the potential benefits of the silencing of Mst1 to improve cardiac function.

Mst1 knockout reduces HP-induced inflammation and oxidative stress. HP is often associated with the increased expression of inflammatory factors in the heart, such as IL-6 and TNF-α (24). Indeed, the present study observed an increase in IL-6 (P<0.05) and TNF-α (P<0.05) expression in the HP group. Both IL-6 and TNF-α expression levels were

decreased in Mst1⁻/⁻ mice in the HP group (both P<0.05, Fig. 2A and B), indicating that the silencing of Mst1 expression can protect against inflammation during HP myocardial injury. In addition, an increase was found in oxidative stress, as evidenced by changes in MDA, SOD and GSH-PX levels (all P<0.05, Fig. 2C-E), similar to the findings of a previous study (25). Of note, a significant increase in MDA, and a decrease in SOD and GSH-PX levels were observed in the HP group (all P<0.05, Fig. 2C-E). Mst1 knockout in the HP group markedly abrogated the HP-mediated induction of these oxidative stress markers (all P<0.05, Fig. 2C-E).
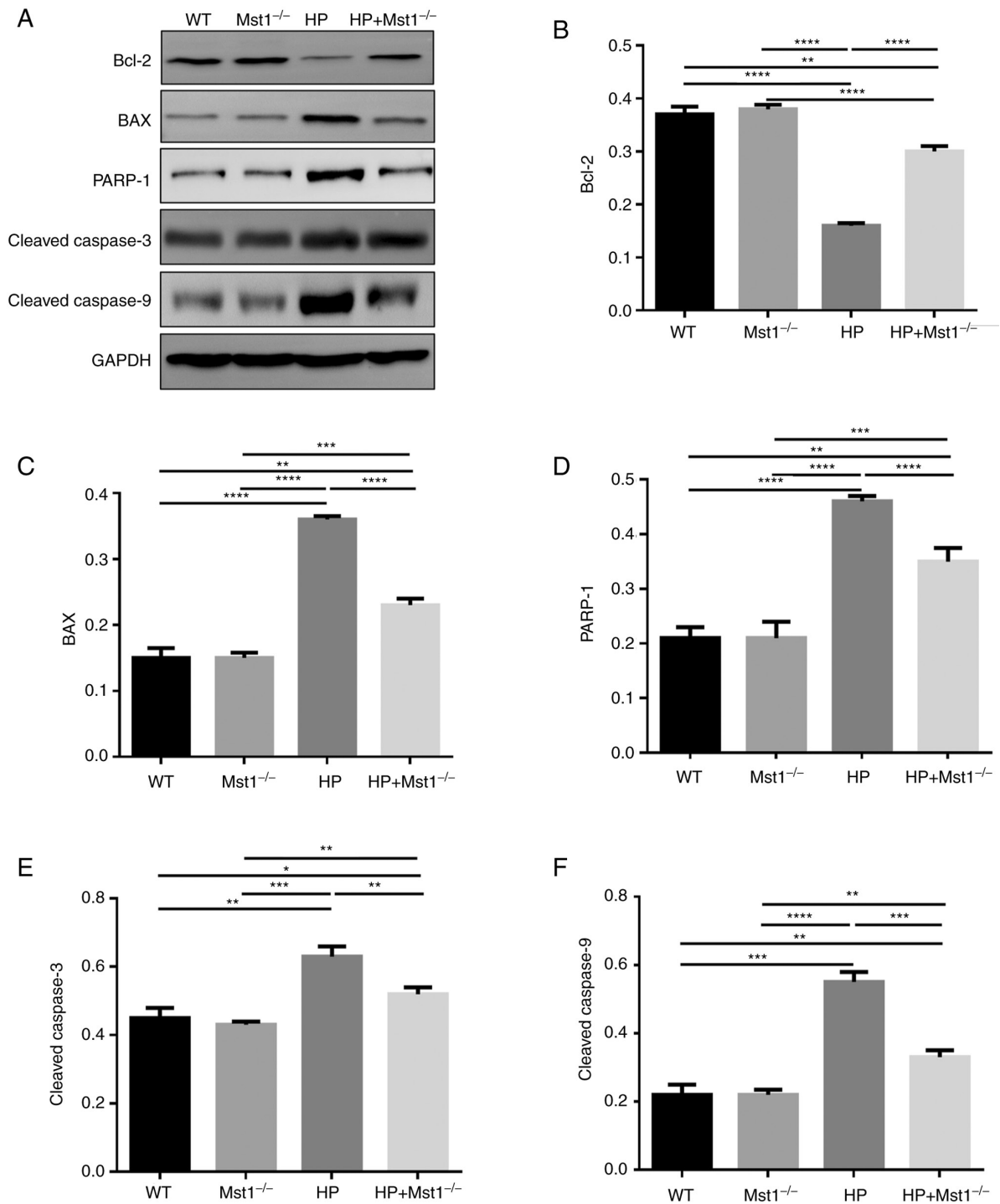
Figure 4. Expression of apoptosis-related proteins. (A) representative western blots. Quantification of the expression level of (B) Bcl-2, (C) BAX, (D) PARP-1, (E) cleaved caspase-3, and (F) cleaved caspase-9 in WT, Mst1^{-/-}, HP and HP Mst1^{-/-} mice. *P<0.05, **P<0.01, ***P<0.001 and ****P<0.0001. WT, wild-type; Mst1, mammalian ste20-like kinase 1; HP, hypertensive/hypertension.

Mst1 knockout decreases HP-induced myocardial apoptosis. A key event in cardiac HP is the apoptosis of cardiomyocytes and CMECs (10,12,26). In the present study, TUNEL staining was used to compare apoptosis in myocardial sections from the different groups. There was a marked increase in the apoptotic ratio in the myocardial tissues in the HP group compared to the non-HP groups (both P<0.05, Fig. 3). As was expected, Mst1 knockout abolished the HP-induced increase in apoptosis in the HP group (both P<0.05, Fig. 3), further confirming the beneficial roles of inhibiting Mst1 in cardiac HP. In addition,

the protein expression levels of apoptosis-related proteins were measured. The expression of Bcl-2 was decreased, while the expression levels of BAX, PARP-1, cleaved caspase-3 and cleaved caspase-9 were increased in the HP group (all P<0.01, Fig 4). However, these changes induced by HP were significantly attenuated in the Mst1^{-/-} mice (all P<0.01, Fig 4).

Mst1-deficient microvascular endothelial cells exhibit an improved integrity and mitochondrial membrane potential in HP models. As microvascular endothelial cell apoptosis
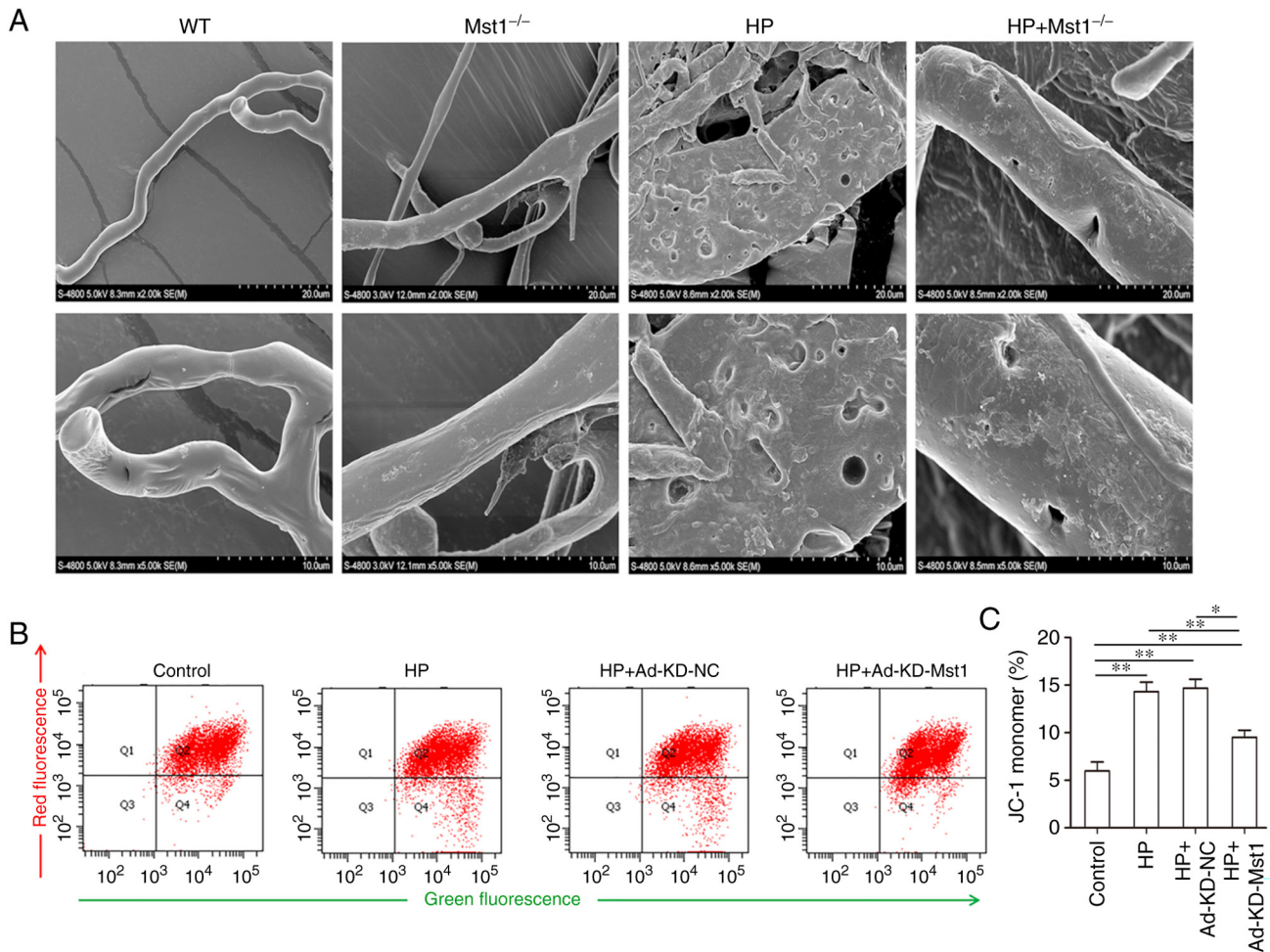
Figure 5. Microvascular endothelial cell integrity and mitochondrial membrane potential of Ang II-treated endothelial cells. (A) Representative scanning electron microscopy images of mouse myocardial microvascular endothelial cells. (B) FACS measurement of mitochondrial membrane potential of CMECs. (C) Quantitative assessment of mitochondrial membrane potential of CMECs; n=3. *P<0.05 and **P<0.01. CMECs, cardiac microvascular endothelial cells; WT, wild-type; Mst1, mammalian ste20-like kinase 1; HP, hypertensive/hypertension; KD, knockdown; NC, negative control.

is critical for endothelial integrity, and in turn for cardiac microcirculation (26), the present study hypothesized that the inhibition of Mst1 may improve myocardial endothelial integrity in HP mice. The microvascular corrosion casting results demonstrated that the microvascular endothelial integrity was severely damaged in the HP group compared to the non-HP groups, and Mst1 knockout efficiently ameliorated the altered endothelial cell integrity (Fig. 5A), consistent with the function of Mst1 in apoptosis. It was then hypothesized that Mst1 could also improve mitochondrial function in HP-compromised myocardial microvascular endothelial cells. It was found that Mst1 knockdown attenuated the disproportion of mitochondrial membrane potential in the HP endothelial cell model (P<0.05, Fig. 5B and C). To summarize, the silencing of Mst1 improved microvascular endothelial cell functions in the heart in HP.

Mst1 deficiency increases autophagy in HP hearts and endothelial cells. The dysregulation of autophagy is frequently associated with cardiac disease, and the balance between autophagy and apoptosis has become a therapeutic target (8,9). Using TEM, the present study found a decrease in the number of autophagosomes in the HP CMECs compared

to the control CMECs, and Mst1 knockdown recovered the number of autophagosomes (Fig. 6A). Fluorescence microscopy detected the expression of the key autophagy markers, p62 and LC3B, in both *in vivo* myocardial tissue sections and *in vitro* CMECs, providing additional evidence that Mst1 silencing can reverse the inhibition of autophagy in cardiac HP *in vivo* (all P<0.05, Fig. 6B-E). These findings suggest that modulating autophagy by inhibiting Mst1 is a critical factor in treating HP injury.

Mst1 plays a critical role in modulating autophagy in the HP heart. To verify the role of Mst1 in the HP heart, the present study then examined the expression and activation of Mst1 and the autophagy markers, Beclin-1, LC3B and p62, in CMECs and cardiac tissues using western blot analysis (all P<0.05, Fig. 7). In both the *in vivo* and *in vitro* HP models, it was observed that Mst1 deficiency, along with blocking its activation, corresponded with the activation of autophagy, reflected by the increased expression of Beclin-1, increased LC3B lipidation and decreased p62 accumulation (all P<0.05, Fig. 7). Together, these results suggest that Mst1 may be a master regulator of autophagy in mouse hearts in HP. Subsequently, Cultured CMECs were treated with 50 nM bafilomycin A1 for 2 h to
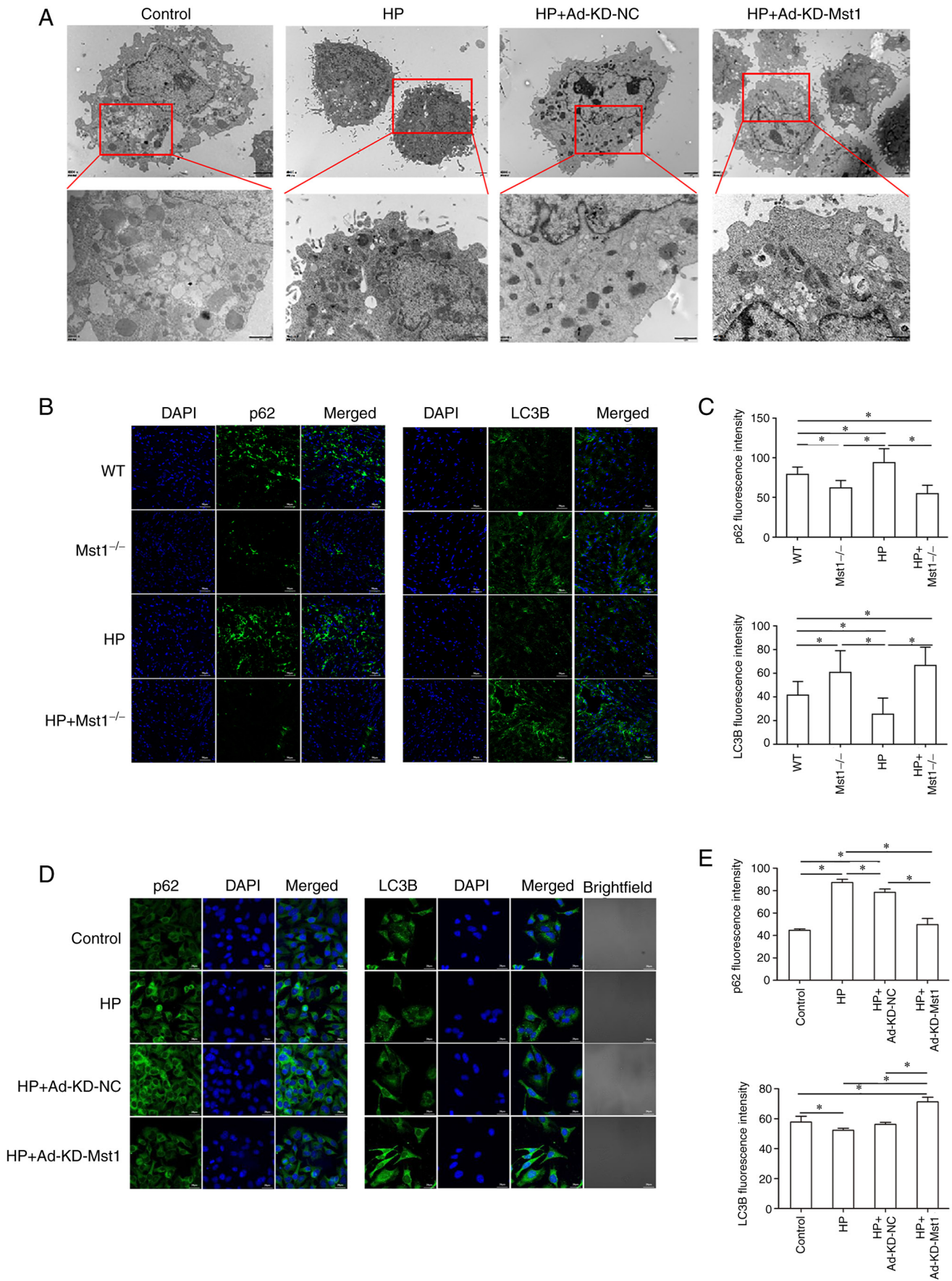
Figure 6. Increased autophagy in Mst1-deficient endothelial cells. (A) TEM images of CMECs. Scale bar, 2 μm. (B) Representative immunofluorescence images of p62 and LC3B in mouse myocardium; magnification, x200. (C) Quantitative assessment of immunofluorescence images; n=3. (D) Representative immunofluorescence images of p62 and LC3B in CMECs; magnification, x200. (E) Quantitative assessment of immunofluorescence images; n=3. *P<0.05. WT, wild-type; Mst1, mammalian ste20-like kinase 1; HP, hypertensive/hypertension; LC3B, microtubule-associated proteins 1A/1B light chain 3B; CMECs, cardiac microvascular endothelial cells; KD, knockdown; NC, negative control.
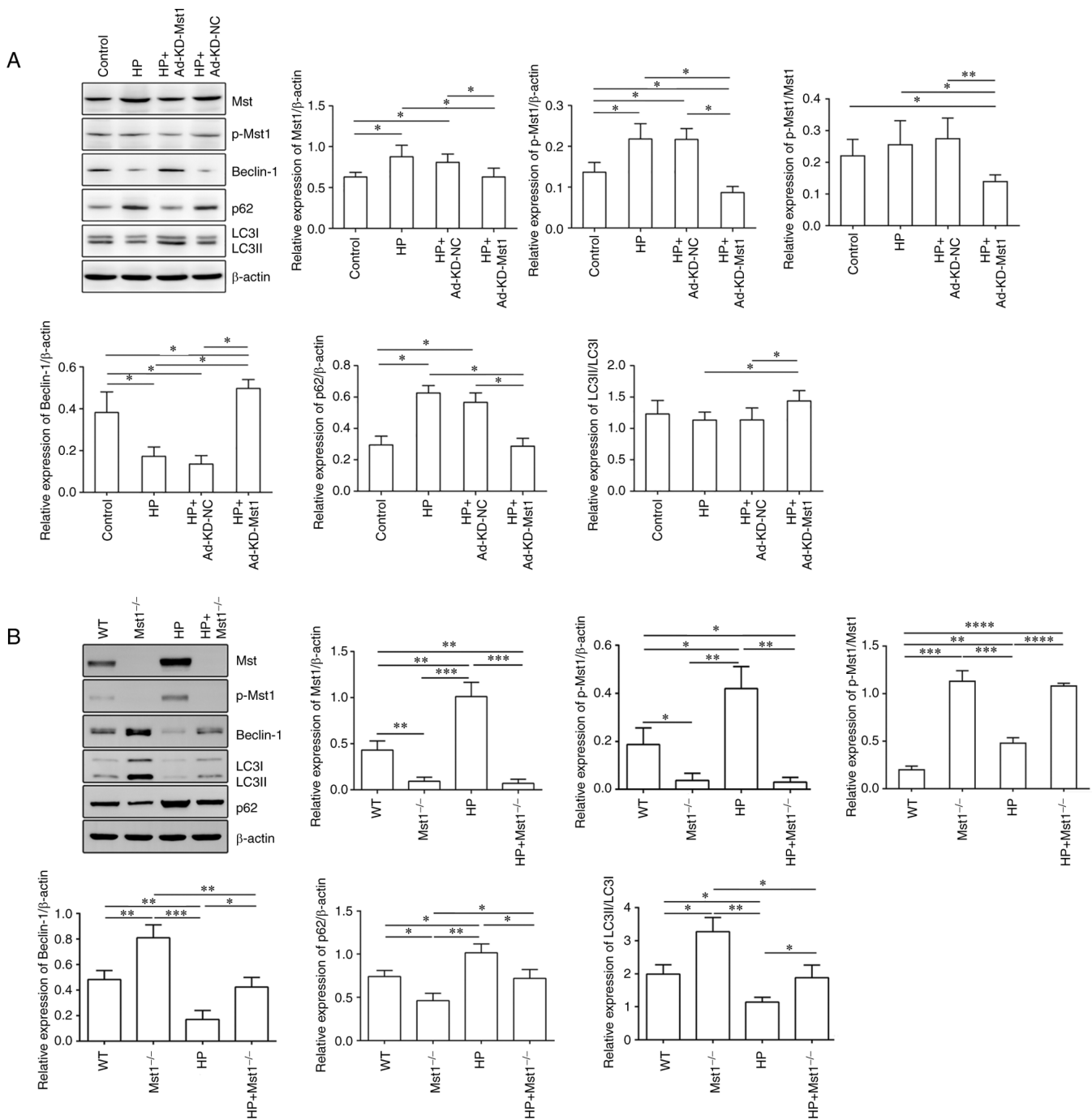
Figure 7. Modulation of core autophagy protein expression by Mst1. (A) Representative western blots of Mst1, p-Mst1, Beclin-1, p62, LC3B and β-actin proteins in CMECs and the quantitative assessment of the western blots; n=4. (B) Representative western blots of Mst1, p-Mst1, Beclin-1, p62, LC3B and β-actin proteins in mouse myocardium and the quantitative assessment of the western blots; n=3. *P<0.05, **P<0.01, ***P<0.001 and ****P<0.0001. Mst1, mammalian ste20-like kinase 1; LC3B, microtubule-associated proteins 1A/1B light chain 3B; CMECs, cardiac microvascular endothelial cells; WT, wild-type; HP, hypertensive/hypertension; KD, knockdown; NC, negative control.

determine the activity of the autophagic flux. Consistently, the enhanced autophagic flux exerted by Mst1 deficiency was demonstrated by an increased LC3 II/LC3 I ratio and a decreased p62 expression in the presence of bafilomycin A1 (Fig. 8).

Discussion

Myocardial remodeling is a compensatory response to HP myocardial injury and is indicated by cardiac hypertrophy, fibrosis, inflammation, mitochondria injury, impaired autophagy and an enhanced apoptosis (3). Severe myocardial remodeling can even lead to arrhythmia and heart failure. The present study demonstrated that Mst1, a protein kinase activated during HP, is a key regulator of HP myocardial injury. The silencing of Mst1 in vivo markedly ameliorated the changes in cardiac structure and function, and reduced inflammation, oxidative stress and the apoptosis of CMECs in the HP mouse model. In addition, Mst1 knockdown in vitro restored endothelial integrity, improved mitochondrial membrane
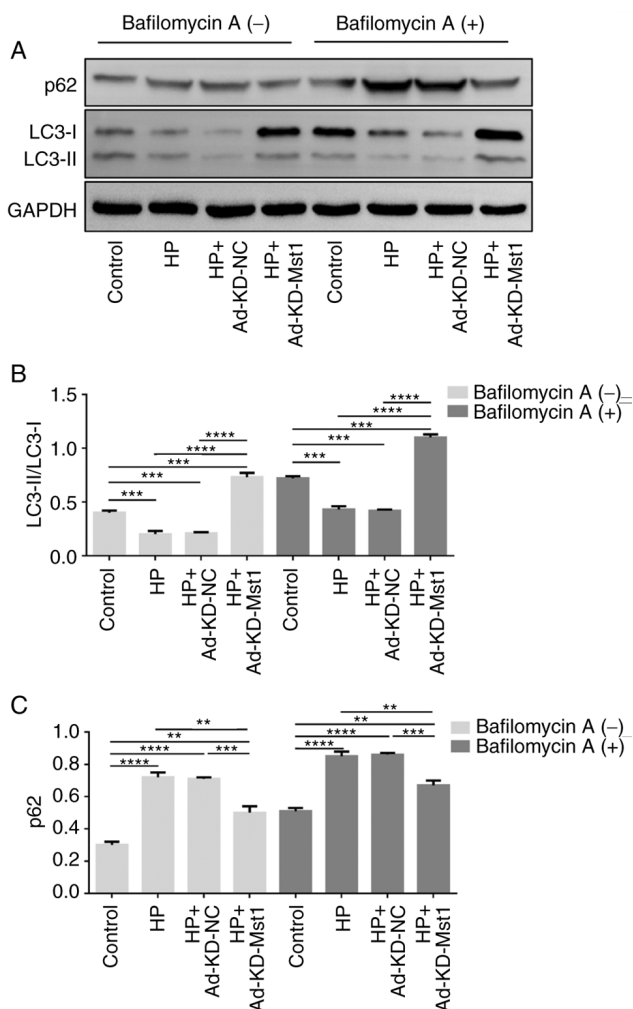
Figure 8. Autophagy-related protein expression with autophagy inhibitors. (A) Representative western blots. Quantification of the expression of (B) LC3B and (C) p62 in CMECs treated with or without bafilomycin A1. **P<0.01, ***P<0.001 and ****P<0.0001. LC3B, microtubule-associated proteins 1A/1B light chain 3B; CMECs, cardiac microvascular endothelial cells; Mst1, mammalian ste20-like kinase 1; HP, hypertensive/hypertension; KD, knockdown; NC, negative control.

potential and activated autophagy, conferring protective effects in the HP cell culture model.

Mst1 has been implicated as a key factor that regulates the balance between apoptosis and autophagy in the cardiovascular system (12,13,16,27,28). Generally, autophagy inhibits the induction of apoptosis, and apoptosis blocks the autophagic process (29). Impaired autophagy and enhanced apoptosis are associated with HP heart disease (6). Therefore, Mst1 may play a role in HP myocardial injury by regulating the balance between autophagy and apoptosis. It has been reported that Mst1 plays a critical role in regulating autophagy by phosphorylating LC3, a marker of autophagy (30-32). In physiological settings, Mst1 is a critical factor in the development of the cardiovascular system, specifically as regards the modulation of cardiomyocyte growth and apoptosis (27). Under pathophysiological conditions, multiple stresses, such as oxidative stress, ischemia and hypoxia, can activate Mst1. The persistent activation of Mst1 has been shown to be associated with a variety of cardiovascular diseases, including DCM, atherosclerosis and ischemia/reperfusion injury (14,33,34).

However, whether Mst1 plays a role in myocardial injury induced by HP remains largely unknown.

In the present study, to investigate the role of Mst1 in HP cardiomyopathy, a HP mouse model was constructed using WT and Mst1$^{-/-}$ mice. The echocardiography results revealed that Mst1 knockout attenuated the HP-induced impairment of cardiac function as indicated by changes in LVFS and LVEF. H&E and Masson's trichrome staining also revealed reduced cardiomyocyte hypertrophy and fibrosis in the Mst1$^{-/-}$ mice compared with the WT mice, indicating that the inhibition of Mst1 improves cardiac function and remodeling *in vivo*. There is evidence to indicate that Ang II-induced pathological cardiac hypertrophy is associated with decreased autophagy (35-38). The findings in the present study suggest that Mst1 may regulate autophagy and attenuate Ang II-induced pathological cardiac hypertrophy in mice.

HP is often associated with the increased expression of inflammatory factors and elevated oxidative stress in the heart (26). The present study demonstrated that in the HP mouse models, Mst1 knockout reduced the expression of IL-6 and TNF-α compared with the WT group, suggesting a protective effect of Mst1 knockout. In addition, less myocardial oxidative stress was observed in the Mst1$^{-/-}$ mice, as indicated by a reduction in MDA and GSH-PX compared with the WT mice.

To further evaluate the function of Mst1 in HP, myocardial apoptosis was measured in the Mst1$^{-/-}$ mice and WT mice using TUNEL assay. As was expected, cardiomyocyte apoptosis increased in the HP group, which was abolished by Mst1 knockout, supporting the protective role of Mst1 in HP-induced cardiomyocyte apoptosis.

The present study also found that Mst1 knockout significantly improved myocardial microvascular endothelial integrity in HP mice, suggesting a role for Mst1 in endothelial cell function, consistent with the findings of a previous study (39). One factor that contributes to HP is the apoptosis of microvascular endothelial cells, as this directly leads to microcirculation reduction and peripheral resistance increase, both of which result in elevated blood pressure (10,40). Microcirculation impairment can also cause organ injury due to a decrease in nutrient and oxygen supply. Therefore, the perturbation of the microcirculation can lead to a range of cardiovascular diseases, such as diabetic cardiomyopathy, atherosclerosis, angina pectoris and ischemia/reperfusion injury (26,41). A previous study found that high glucose can phosphorylate and activate Mst1 in myocardial microvascular endothelial cells, promote apoptosis, and inhibit autophagy, resulting in diabetic cardiomyopathy (12).

Mitochondrial membrane potential reflects mitochondrial function, and its dysregulation can initiate apoptosis (42). The present study assessed mitochondrial membrane potential in CMECs using JC-1 staining and observed that the knockdown of Mst1 *in vitro* markedly reversed the Ang II-induced increase in membrane potential, demonstrating a beneficial effect of inhibiting Mst1 on mitochondrial health.

Physiological autophagy is a key mechanism in the quality control of proteins and organelles and therefore, in cell homeostasis (7,8). The dysregulation of autophagy under conditions of stress is frequently implicated in heart diseases (43). Using TEM, the present study observed a marked increase in the

number of autophagosomes in the Mst1-deficient mouse myocardial microvascular endothelial cells compared with the WT cells following the induction of HP. Fluorescence microscopy and western blot analysis of the autophagy markers, p62 and LC3B, further confirmed that the silencing of Mst1 increased autophagy in both the *in vivo* and *in vitro* HP models.

In the heart, constitutive autophagy is not only a homeostatic mechanism for maintaining cardiac structure and function, but is also of utmost importance for the maintenance of cardiac cellular integrity. However, the disruption of autophagy may lead to heart failure (44). The findings of the present study suggest that Mst1 plays roles in the regulation of autophagy, apoptosis, oxidative stress and inflammation in HP hearts. A possible mechanism involved is that the loss of Mst1 primarily induces protective autophagy, which subsequently inhibits apoptosis, oxidative stress and inflammatory responses, leading to suppressed cardiomyocyte injury in HP. This hypothesis warrants investigation in future studies. In summary, Mst1 inhibition can considerably ameliorate HP-induced myocardial injury which is associated with enhanced microvascular endothelial cell autophagy and decreased apoptosis. Mst1$^{-/-}$ mice were used in the present study, while further studies are required in the future to determine whether the inhibition or downregulation of Mst1 using pharmacological approaches prevents or improves myocardial injury induced by HP. The promising beneficial effects of Mst1 silencing may provide novel strategies for the treatment of HP heart diseases.

Acknowledgements

Funding

Availability of data and materials

The datasets generated and analyzed during the present study are available from the corresponding author upon reasonable request.

Authors' contributions

LPW was involved in the conceptualization of the study, and in the provision of data analysis and funding support. RMH, BW and XX were involved in data curation and in the study methodology. MYL, YHD, WW and CH were involved in the experiment operation and data analysis. JL was involved in the conceptualization of the study, as well as in data curation, formal analysis, funding acquisition, the study methodology, project administration, the provision of funding support, in the writing of the original draft, and in the writing, reviewing and editing of the manuscript. JL and LPW confirmed the authenticity of all the raw data. All authors have read and approved the final manuscript.

Ethics approval and consent to participate

The present study was reviewed and approved by the Ethics Committee of The First Affiliated Hospital, Xinjiang Medical University (approval no. IACUC20201116-13). All procedures performed involving animals were in accordance with the ethical standards of the institution or practice at which the studies were conducted.

Patient consent for publication

Not applicable.

Competing interests

The authors declare that they have no competing interests.

References

1. Oparil S, Acelajado MC, Bakris GL, Berlowitz DR, Cífková R, Dominiczak AF, Grassi G, Jordan J, Poulter NR, Rodgers A and Whelton PK: Hypertension. Nat Rev Dis Primers 4: 18014, 2018.
2. McCormack T, Krause T and O'Flynn N: Management of hypertension in adults in primary care: NICE guideline. Br J Gen Pract 62: 163-164, 2012.
3. Gonzalez A, Ravassa S, Lopez B, Moreno MU, Beaumont J, José GS, Querejeta R, Bayés-Genís A and Díez J: Myocardial remodeling in hypertension. Hypertension 72: 549-558, 2018.
4. Gobé G, Browning J, Howard T, Hogg N, Winterford C and Cross R: Apoptosis occurs in endothelial cells during hypertension-induced microvascular rarefaction. J Struct Biol 118: 63-72, 1997.
5. White K, Dempsie Y, Caruso P, Wallace E, McDonald RA, Stevens H, Hatley ME, Rooij EV, Morrell NW, MacLean MR and Baker AH: Endothelial apoptosis in pulmonary hypertension is controlled by a microRNA/programmed cell death 4/caspase-3 axis. Hypertension 64: 185-194, 2014.
6. Wang ZV, Rothermel BA and Hill JA: Autophagy in hypertensive heart disease. J Biol Chem 285: 8509-8514, 2010.
7. Sciarretta S, Maejima Y, Zablocki D and Sadoshima J: The role of autophagy in the heart. Annu Rev Physiol 80: 1-26, 2018.
8. Nemchenko A, Chiong M, Turer A, Lavandero S and Hill JA: Autophagy as a therapeutic target in cardiovascular disease. J Mol Cell Cardiol 51: 584-593, 2011.
9. Wang F, Jia J and Rodrigues B: Autophagy, metabolic disease, and pathogenesis of heart dysfunction. Can J Cardiol 33: 850-859, 2017.
10. Savoia C, Battistoni A, Calvez V, Cesario V, Montefusco G and Filippini A: Microvascular alterations in hypertension and vascular aging. Curr Hypertens Rev 13: 16-23, 2017.
11. Wu B, Lin J, Luo J, Han D, Fan M, Guo T, Tao L, Yuan M and Yi F: Dihydromyricetin protects against diabetic cardiomyopathy in streptozotocin-induced diabetic mice. Biomed Res Int 2017: 3764370, 2017.
12. Zhang M, Zhang L, Hu J, Lin J, Wang T, Duan Y, Man W, Feng J, Sun L, Jia H, et al: MST1 coordinately regulates autophagy and apoptosis in diabetic cardiomyopathy in mice. Diabetologia 59: 2435-2447, 2016.
13. Maejima Y, Kyoi S, Zhai P, Liu T, Li H, Ivessa A, Sciarretta S, Re DPD, Zablocki DK, Hsu CP, et al: Mst1 inhibits autophagy by promoting the interaction between Beclin1 and Bcl-2. Nat Med 19: 1478-1488, 2013.
14. Yamamoto S, Yang G, Zablocki D, Liu J, Hong C, Kim SJ, Soler S, Odashima M, Thaisz J, Yehia G, et al: Activation of Mst1 causes dilated cardiomyopathy by stimulating apoptosis without compensatory ventricular myocyte hypertrophy. J Clin Invest 111: 1463-1474, 2003.

15. Foulquier S, Namsolleck P, Van Hagen BT, Milanova I, Post MJ, Blankesteijn WM, Rutten BP, Prickaerts J, Van Oostenbrugge RJ and Unger T: Hypertension-induced cognitive impairment: Insights from prolonged angiotensin II infusion in mice. Hypertens Res 41: 817-827, 2018.
16. Cheng Z, Zhang M, Hu J, Lin J, Feng X, Wang S, Wang T, Gao E, Wang H and Sun D: Mst1 knockout enhances cardiomyocyte autophagic flux to alleviate angiotensin II-induced cardiac injury independent of angiotensin II receptors. J Mol Cell Cardiol 125: 117-128, 2018.
17. Froese N, Kattih B, Breitbart A, Grund A, Geffers R, Molkentin JD, Kispert A, Wollert KC, Drexler H and Heineke J: GATA6 promotes angiogenic function and survival in endothelial cells by suppression of autocrine transforming growth factor beta/activin receptor-like kinase 5 signaling. J Biol Chem 286: 5680-5690, 2011.
18. Lu Y, Wang RH, Guo BB and Jia YP: Quercetin inhibits angiotensin II induced apoptosis via mitochondrial pathway in human umbilical vein endothelial cells. Eur Rev Med Pharmacol Sci 20: 1609-1616, 2016.
19. He TC, Zhou S, da Costa LT, Yu J, Kinzler KW and Vogelstein B: A simplified system for generating recombinant adenoviruses. Proc Natl Acad Sci USA 95: 2509-2514, 1998.
20. Van De Vlekkert D, Machado E and d'Azzo A: Analysis of generalized fibrosis in mouse tissue sections with Masson's Trichrome staining. Bio Protoc 10: e3629, 2020.
21. Van Steenkiste C, Trachet B, Casteleyn C, van Loo D, Hoorebeke LV, Segers P, Geerts A, Vlierberghe HV and Colle I: Vascular corrosion casting: Analyzing wall shear stress in the portal vein and vascular abnormalities in portal hypertensive and cirrhotic rodents. Lab Invest 90: 1558-1572, 2010.
22. De Biasi S, Gibellini L and Cossarizza A: Uncompensated polychromatic analysis of mitochondrial membrane potential using JC-1 and multilaser excitation. Curr Protoc Cytom 72: 7.32.1-7.32.11, 2015.
23. Arai R and Waguri S: Improved electron microscopy fixation methods for tracking autophagy-associated membranes in cultured mammalian cells. Methods Mol Biol 1880: 211-221, 2019.
24. Tomiyama H, Shiina K, Matsumoto-Nakano C, Ninomiya T, Komatsu S, Kimura K, Chikamori T and Yamashina A: The contribution of inflammation to the development of hypertension mediated by increased arterial stiffness. J Am Heart Assoc 6: e005729, 2017.
25. Kuyumcu F and Aycan A: Evaluation of oxidative stress levels and antioxidant enzyme activities in burst fractures. Med Sci Monit 24: 225-234, 2018.
26. Suematsu M, Suzuki H, Delano FA and Schmid-Schonbein GW: The inflammatory aspect of the microcirculation in hypertension: Oxidative stress, leukocytes/endothelial interaction, apoptosis. Microcirculation 9: 259-276, 2002.
27. Yang Y, Wang H, Ma Z, Hu W and Sun D: Understanding the role of mammalian sterile 20-like kinase 1 (MST1) in cardiovascular disorders. J Mol Cell Cardiol 114: 141-149, 2018.
28. Feng X, Wang S, Yang X, Lin J, Man W, Dong Y, Zhang Y, Zhao Z, Wang H and Sun D: Mst1 knockout alleviates mitochondrial fission and mitigates left ventricular remodeling in the development of diabetic cardiomyopathy. Front Cell Dev Biol 8: 628842, 2020.
29. Marino G, Niso-Santano M, Baehrecke EH and Kroemer G: Self-consumption: The interplay of autophagy and apoptosis. Nat Rev Mol Cell Biol 15: 81-94, 2014.
30. Wilkinson DS, Jariwala JS, Anderson E, Mitra K, Meisenhelder J, Chang JT, Ideker T, Hunter T, Nizet V, Dillin A and Hansen M: Phosphorylation of LC3 by the Hippo kinases STK3/STK4 is essential for autophagy. Mol Cell 57: 55-68, 2015.
31. Nieto-Torres JL, Shanahan SL, Chassefeyre R, Chaiamarit T, Zaretski S, Landeras-Bueno S, Verhelle A, Encalada SE and Hansen M: LC3B phosphorylation regulates FYCO1 binding and directional transport of autophagosomes. Curr Biol 31: 3440-3449 e3447, 2021.
32. Nieto-Torres JL, Encalada SE and Hansen M: LC3B phosphorylation: Autophagosome's ticket for a ride toward the cell nucleus. Autophagy 17: 3266-3268, 2021.
33. Yu W, Xu M, Zhang T, Zhang Q and Zou C: Mst1 promotes cardiac ischemia-reperfusion injury by inhibiting the ERK-CREB pathway and repressing FUNDC1-mediated mitophagy. J Physiol Sci 69: 113-127, 2019.
34. Wang T, Zhang L, Hu J, Duan Y, Zhang M, Lin J, Man W, Pan X, Jiang Z, Zhang G, *et al*: Mst1 participates in the atherosclerosis progression through macrophage autophagy inhibition and macrophage apoptosis enhancement. J Mol Cell Cardiol 98: 108-116, 2016.
35. Mehta PK and Griendling KK: Angiotensin II cell signaling: Physiological and pathological effects in the cardiovascular system. Am J Physiol Cell Physiol 292: C82-C97, 2007.
36. Li AL, Lv JB and Gao L: MiR-181a mediates Ang II-induced myocardial hypertrophy by mediating autophagy. Eur Rev Med Pharmacol Sci 21: 5462-5470, 2017.
37. Kishore R, Krishnamurthy P, Garikipati VN, Benedict C, Nickoloff E, Khan M, Johnson J, Gumpert AM, Koch WJ and Verma SK: Interleukin-10 inhibits chronic angiotensin II-induced pathological autophagy. J Mol Cell Cardiol 89: 203-213, 2015.
38. Zhou L, Ma B and Han X: The role of autophagy in angiotensin II-induced pathological cardiac hypertrophy. J Mol Endocrinol 57: R143-R152, 2016.
39. Qin R, Lin D, Zhang L, Xiao F and Guo L: Mst1 deletion reduces hyperglycemia-mediated vascular dysfunction via attenuating mitochondrial fission and modulating the JNK signaling pathway. J Cell Physiol 235: 294-303, 2020.
40. Dong Q, Xing W, Su F, Liang X, Tian F, Gao F, Wang S and Zhang H: Tetrahydroxystilbene glycoside improves microvascular endothelial dysfunction and ameliorates obesity-associated hypertension in obese ZDF rats via inhibition of endothelial autophagy. Cell Physiol Biochem 43: 293-307, 2017.
41. Wang B, Li BW, Li HW, Li AL, Yuan XC, Wang Q and Xiu RJ: Enhanced matrix metalloproteinases-2 activates aortic endothelial hypermeability, apoptosis and vascular rarefaction in spontaneously hypertensive rat. Clin Hemorheol Microcirc 57: 325-338, 2014.
42. Zorova LD, Popkov VA, Plotnikov EY, Silachev DN, Pevzner IB, Jankauskas SS, Babenko VA, Zorov SD, Balakireva AV, Juhaszova M, *et al*: Mitochondrial membrane potential. Anal Biochem 552: 50-59, 2018.
43. Yan L, Vatner DE, Kim SJ, Ge H, Masurekar M, Massover WH, Yang G, Matsui Y, Sadoshima J and Vatner SF: Autophagy in chronically ischemic myocardium. Proc Natl Acad Sci USA 102: 13807-13812, 2005.
44. Nah J, Fernandez AF, Kitsis RN, Levine B and Sadoshima J: Does autophagy mediate cardiac myocyte death during stress? Circ Res 119: 893-895, 2016.